

# Small Perturbation Harmonic Coupling in Nonlinear Periodicity Preservation Circuits

Charles Baylis, II, *Member, IEEE*, and Robert J. Marks, II, *Fellow, IEEE*

**Abstract**—Nonlinear systems and circuits, while required for many applications, presently require a design procedure that is often complex. In many cases, the design process is either based upon measurements or complex nonlinear models. This paper presents periodicity preservation (PP) and time invariant PP (TIPP) system theory as a simple way to characterize behavior for a significant class of nonlinear systems. PP systems preserve signal periodicity and are conducive to modeling harmonic coupling. When linearized to small perturbations, the harmonic coupling is described by the Jacobian about the operating point. The harmonic coupling weights, which are elements of the Jacobian, can be measured experimentally. For some TIPP systems such as LTI systems and memoryless nonlinearities, a single experiment suffices to determine the harmonic coupling weights. Other PP systems, including mixing and linear time variant systems, require more experimental queries. TIPP system theory is foundational to the theory of X-parameters®, S-functions and polyharmonic distortion.

**Index Terms**—Affine approximation, harmonic coupling, harmonics, nonlinear systems, power amplifier design, Wirtinger calculus.

## I. INTRODUCTION

IN disciplines requiring amplifiers, such as wireless, aerospace [1]–[3], radar [4] commercial communications [5], and electronic devices [6]–[8] we can be required to operate in nonlinear regimes to provide adequate output power for required performance. As circuits are driven into nonlinear regions of operation, the signal spectrum expands based on the harmonic coupling characteristics of the system. Understanding the nonlinearities of the system, as manifested in the harmonic coupling, can be essential in understanding perturbations about the operating point. In the wireless area, for example, tighter regulatory constraints for the spectrum are being placed on both wireless communications and radar due to the increasing demand for bandwidth for broadband wireless systems and applications [1]. The desire to conserve energy by operating amplifiers with higher efficiency decreases the linearity of the amplifier. As the amplifier becomes nonlinear, the harmonic transfer characteristics of the system cause expansion of the

spectrum due to intermodulation. As a result, being able to predict the harmonic coupling of a nonlinear DUT is important in many applications. Harmonic distortion [3], [9] including AM/AM and AM/PM distortion [10] are examples. In power and energy systems, nonlinear power converters often create significant amounts of harmonic distortion, causing “dirty” power to be generated. Understanding the nonlinearities of the power converter systems can allow analysis and potential development of compensation methodologies for the nonlinearities, allowing cleaner power signals to be generated. In a variety of signal processing and waveform diversity applications, the ability to adjust a waveform to compensate for system nonlinearities is also an expected useful result from accurate characterization of nonlinear systems.

Groundbreaking nonlinear system harmonic coupling characterizations [11]–[15] such as VIOMAP [15], S-functions [16]–[20], polyharmonic distortion (PHD) models [22]–[27] and X-parameters® [28]–[39] have been offered as approaches to the “black-box” modeling of nonlinear devices. They differ from more traditional nonlinear models such as those of Volterra & Norbert Wiener [40]–[45] and Hermite [46]. The PP model is applicable to small periodic input perturbations and allows characterization using straightforward harmonic measurements that can be performed in the laboratory. These models have been shown to be effective tools for predicting the nonlinear behavior of RF front end systems in simulations. X-parameters® are measured by Agilent’s PNA-X series of microwave network analyzers.

Our presentation of harmonic coupling uses a single input-single output system configuration. In the sense  $z$  parameters can be viewed as consisting of two Thevinin circuits coupled with dependent voltage sources [47], the single port characterization can be extended straightforwardly to two or more ports [7].

Linear time-invariant (LTI) systems have a rich theoretical foundation from which insightful characterization can be extracted. Despite their widespread use, there exists no similar foundational, “from first principles” model from which the harmonic characterization of nonlinear systems are made. In this paper, we propose such a theory for one port networks where signal periodicity is preserved.

## II. FOUNDATIONS

We denote a nonlinear system by the operator  $\mathbf{Z}$  so that

$$v(t) = \mathbf{Z}\{i(t)\} \quad (1)$$

where  $i(t)$  is the stimulus and  $v(t)$  is the response. The operator  $\mathbf{Z}$  is general in the sense that it can represent in principle,

Manuscript received December 28, 2011; revised April 01, 2012; accepted April 21, 2012. Date of publication July 25, 2012; date of current version November 21, 2012. This work was supported by a grant from the U.S. Naval Research Laboratory. A tutorial introduction to this material has been presented by the authors in IEEE Microwave Magazine [7]. This paper was recommended by Associate Editor I. Belykh.

The authors are with the Wireless and Microwave Circuits and Systems Program, Department of Electrical and Computer Engineering Department, Baylor University, Waco, TX 76706 USA (e-mail: Robert\_Marks@baylor.edu).

Digital Object Identifier 10.1109/TCSI.2012.2206438

for example, a wideband system, a system with memory, time variant systems, narrowband systems and even noncausal nonlinear systems.

Consider, then, the perturbation of a nonlinear system operation about the operating point in (1) to  $v_{\Delta}(t) := \mathbf{Z}\{i(t) + \Delta i(t)\}$ . If the nonlinear operator is sufficiently smooth about the operating point we can make the affine approximation

$$v_{\Delta}(t) \simeq \mathbf{Z}\{i(t)\} + \int_{-\infty}^{\infty} \frac{\partial v(t)}{\partial i(\tau)} \Delta i(\tau) d\tau = v(t) + \Delta v(t) \quad (2)$$

where the partial derivative is taken at the operating point. The term  $(\partial v(t))/(\partial i(\tau))$  can be viewed as the contribution of a differential stimulus,  $\partial i(t)$ , at  $t = \tau$  to an incremental change in the response. The weighted super-position of these contributions are then used to approximate the entire perturbation response, i.e.,

$$\Delta v(t) = \int_{-\infty}^{\infty} \frac{\partial v(t)}{\partial i(\tau)} \Delta i(\tau) d\tau. \quad (3)$$

The term  $(\partial v(t))/(\partial i(\tau))$  is the Jacobian of the transformation. Circuit Jacobians are commonly used to perform harmonic load balance [43], [48], [49].

Define

$$V(u) = \mathcal{F}(v(t)) = \int_{-\infty}^{\infty} v(t) e^{-j2\pi ut} dt \quad (4)$$

where  $\mathcal{F}$  denotes Fourier transformation. The inverse transform of (4) is

$$v(t) = \int_{-\infty}^{\infty} V(u) e^{j2\pi ut} du. \quad (5)$$

The superposition in (3) can be represented in different mixtures of time and frequency Jacobians.

$$\Delta v(t) = \int_{-\infty}^{\infty} \frac{\partial v(t)}{\partial I(\nu)} \Delta I(\nu) d\nu \quad (6)$$

$$\Delta V(u) = \int_{-\infty}^{\infty} \frac{\partial V(u)}{\partial i(\tau)} \Delta i(\tau) d\tau \quad (7)$$

$$= \int_{-\infty}^{\infty} \frac{\partial V(u)}{\partial I(\nu)} \Delta I(\nu) d\nu. \quad (8)$$

The four Jacobians are related by Fourier transforms. The relationship among the Jacobians is shown in Fig. 1. Detail derivation of (6) through (8) and the entries in Fig. 1 are in Appendix A. Unconnected nodes in Fig. 1 are related by a two dimensional Fourier transform. For example

$$\frac{\partial V(u)}{\partial i(\tau)} = \int_{-\infty}^{\infty} \int_{-\infty}^{\infty} \frac{\partial v(t)}{\partial I(\nu)} e^{-j2\pi(ut+\nu\tau)} dt d\nu.$$

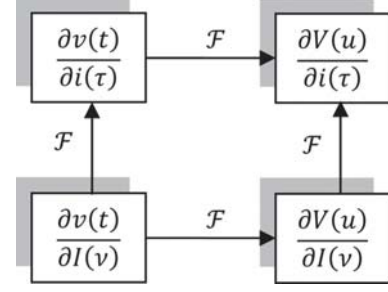


Fig. 1. The four Jacobians in time and frequency and their relationships using Fourier transforms. The Fourier transform arrow depicts a negative sign on the exponent of the Fourier transform kernel as in (4).

*Theorem 1: Linear Systems:* For linear systems [50]–[53], the Jacobian characterization in (3) and (6) through (8) are exact. Furthermore, for linear systems the Jacobian is equal to the impulse response of the possibly time variant [54]–[57] system, i.e.,

$$\frac{\partial v(t)}{\partial i(\tau)} = h(t, \tau) = \mathbf{Z}\{\delta(t - \tau)\}$$

where  $\delta(t)$  is the Dirac delta. The proof is in Appendix B.

*Example 1:* Let

$$v(t) = \int_{-\infty}^t i\left(\frac{\xi}{M}\right) e^{-(t\xi)^2} d\xi$$

where  $M > 0$  is a scaling constant. The system is linear, time variant, and

$$\frac{\partial v(t)}{\partial i(\tau)} = h(t, \tau) = M\mu(Mt - \tau) e^{-(Mt\tau)^2}$$

where the unit step is  $\mu(\xi) = 1$  for  $\xi \geq 0$  and zero otherwise.

Although the system operator  $\mathbf{Z}$  is applicable to many nonlinearities, it takes on a convenient form when the system has no memory.

*Theorem 2: Memoryless Nonlinearities:* Consider the nonlinearity be defined by a memoryless nonlinearity  $g(\cdot)$  i.e.,

$$v(t) = g(i(t)). \quad (9)$$

Then

$$\frac{\partial v(t)}{\partial i(\tau)} = \dot{g}(i(t)) \delta(t - \tau) \quad (10)$$

and

$$\Delta v(t) = \dot{g}(i(t)) \Delta i(t). \quad (11)$$

*Proof:* The result in (10) follows immediately from the chain rule of differential calculus using  $(\partial i(t))/(\partial i(\tau)) = \delta(t - \tau)$ . Then (11) follows from (3).

*Example 2: Exponential Nonlinearity:* To illustrate affine modeling of a memoryless nonlinear system in continuous time, let

$$g(x) = V_0 e^{\rho x} \quad (12)$$

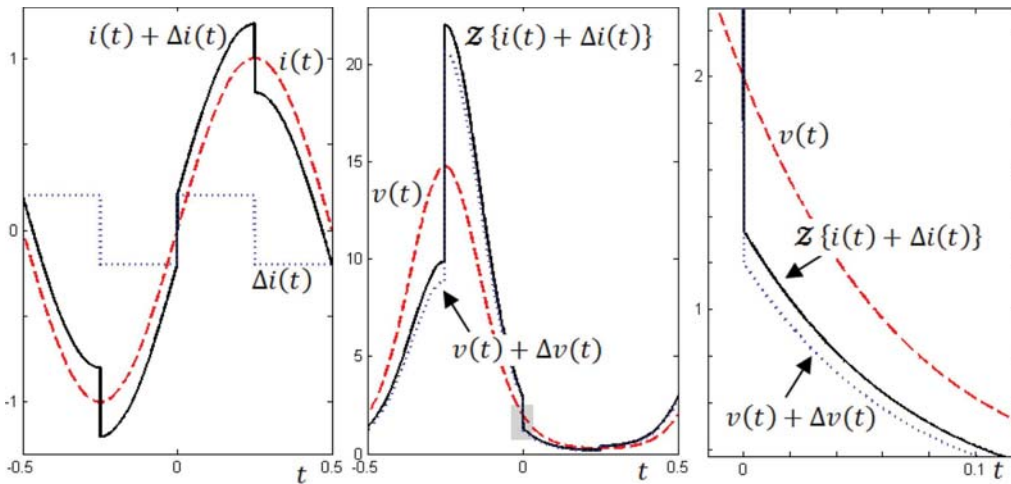


Fig. 2. Affine approximation of the exponential nonlinearity in (12) for  $\rho = -2$ ,  $V_0 = 2$ , and  $i(t)$  equal to the unit period sinusoid shown in the left plot with a dashed line. The perturbation,  $\Delta i(t)$ , is the square wave shown on the left as is the sum  $i(t) + \Delta i(t)$ . In the middle plot is shown the unperturbed output,  $v(t)$ , the true output,  $v_\Delta(t) = \mathcal{Z}\{i(t) + \Delta i(t)\}$ , and the affine approximation  $v(t) + \Delta v(t)$  where  $\Delta v(t)$  is given in (13). On the right is a close-up of the shaded region in the middle plot.

so that

$$v(t) = \mathcal{Z}\{i(t)\} = g(i(t)) = V_0 e^{\rho i(t)}$$

where  $\rho$  and  $V_0$  are real constants. Since  $\dot{g}(i(t)) = \rho v(t)$ , (11) becomes

$$\Delta v(t) = \rho v(t) \Delta i(t). \quad (13)$$

An example of this affine approximation is shown in Fig. 2. Even though the perturbation is a significant percentage of amplitude of the operating point signal, the affine approximation is seen graphically to give a fair characterization.

### III. PERIODICITY PRESERVATION SYSTEMS

A linear time-invariant LTI system, when stimulated by a sinusoidal source will have all of its voltages and currents oscillating at the same frequency albeit at different magnitudes and phases. Phasor analysis, a staple of undergraduate engineering education, keeps track of these two quantities. A generalization of this class is *periodicity preservation* (PP) systems. When stimulated by a periodic stimulus every voltage and current within the system oscillates periodically with the same period as the stimulus.

A signal,  $i(t)$ , is periodic if there exists a period,  $T$ , such that  $i(t) = i(t + T)$  for all  $t$ . The system defined in (1) is PP if the response,  $v(t)$ , is periodic with period,  $T$ , for all periodic stimuli with period,  $T$ . A system can be PP for all periods as is the case for a memoryless nonlinearity, or for a single period as is the case when the system contains an independent periodic source.

For small perturbations in the stimulus, the response perturbation can be estimated using experimentally generated *harmonic coupling weights* (HCWs).

The Fourier series [52] of a periodic signal  $i(\tau)$  is

$$i(\tau) = \sum_{m=-\infty}^{\infty} i_m e^{j2\pi m\tau/T} \quad (14)$$

where  $T$  is the signal's period. The Fourier series coefficients are

$$i_m = \frac{1}{T} \int_T i(\tau) e^{-j2\pi m\tau/T} d\tau \quad (15)$$

and  $\int_T$  means integration over any period of  $i(\tau)$ .

Here are examples of some familiar systems that are PP and the relationship between the input and output Fourier series coefficients.

- **Addition.** Let  $w(t)$  denote a periodic function with the same period,  $T$ , and with Fourier coefficients  $w_n$ . If  $v(t) = i(t) + w(t)$ , then  $v(t)$  has coefficients  $v_n = i_n + w_n$ .
- **Linear Systems.** As we will show in Theorem 3, for time variant linear PP systems, the harmonic coupling weights can be derived from the knowledge of the system impulse response,  $h(t, \tau)$ .
- **Filtering.** Let  $h(t)$  denote an arbitrary impulse response of an LTI system. If  $v(t) = i(t) * h(t)$ , then the Fourier coefficients of  $i(t)$  are multiplied by the system frequency response, i.e., they are equal to  $v_n = i_n H(n/T)$  where  $H(u)$  is the Fourier transform [40] as in (4). The harmonic coupling is then as shown on the left in Fig. 3. There is no harmonic cross coupling. The system impulse response, which can be measured in a single experiment, therefore completely characterizes the harmonic coupling weights.
- **Memoryless Nonlinearity:** Let  $g(\cdot)$  denote an arbitrary function. If  $v(t) = g(i(t))$ , then the Fourier coefficients of  $v(t)$  are

$$v_n = \frac{1}{T} \int_0^T g(i(t)) e^{-j2\pi nt/T} dt. \quad (16)$$

Only higher integer harmonics are generated. The second harmonic of the input, for example, can contribute only to the even harmonics of the response. A sagittal diagram of the harmonic coupling in this case is represented in the middle of Fig. 3.

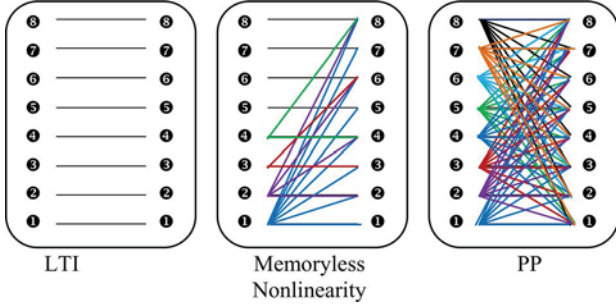


Fig. 3. Saggital diagrams of cross harmonic coupling for the first 8 harmonics for (left) LTI systems, (middle) memoryless nonlinear systems, and (right) general PP systems. The left side denotes the harmonic count of the stimulus and the right the response harmonic to which contributions are made. In the most general PP case, shown on the right, the harmonic coupling can be exhaustive.

- **Mixers:** If  $v(t) = w(t)i(t)$ , then the Fourier series coefficients of  $v(t)$  are the discrete convolution of the Fourier coefficients of the two signals

$$v_n = \sum_{m=-\infty}^{\infty} i_m \omega_{n-m}.$$

As shown on the right in Fig. 3, mixing (multiplying) sinusoids can create harmonics and subharmonics. A cosine with frequency  $3f_0$  multiplied by another with frequency  $2f_0$ , for example, will produce as a component a beat frequency sinusoid with lower frequency  $f_0$ .

All cascading, multiplicative and additive combinations of PP operations likewise constitutes a PP system.

Examples of linear time variant mappings that are not PP systems include coordinate distortion, e.g.,  $v(t) = i(t^3)$  and many integral transforms [52], [53], e.g., a Laplace transform [52], [58], [59]  $v(t) = \int_0^{\infty} i(\tau)e^{-t\tau} d\tau$  and the Mellin transform [52], [60], [61],  $v(t) = \int_0^{\infty} i(\tau)\tau^{t-1} d\tau$ .

#### IV. HARMONIC COUPLING IN PP SYSTEMS

Harmonic coupling in PP systems addresses the manner in which the harmonics of stimulus perturbations contribute to the harmonic changes in the response. A periodic stimulus with Fourier series coefficients  $i_m$  is shown in Fig. 4(a). The response is a periodic signal with Fourier coefficients  $v_n$ . This defines the operating point of the nonlinear mapping. When the input is perturbed to a signal with Fourier series coefficients  $i_m + \Delta i_m$  as shown in Fig. 4(b), the response is periodic with coefficients  $v_n + \Delta v_n$ . Harmonic coupling determines the impact of the input perturbation  $\Delta i_m$  on the output perturbation  $\Delta v_n$ . For small perturbations, the harmonic coupling can be expressed through an affine approximation.

Affine modeling of perturbations of PP systems follows a Jacobian characterization similar to (2), except that mapping is considered only over a period, say  $0 \leq t < T$ . Perturbation of the PP system is limited to periodic signals that are the same period as the operating point. Instead of (2), for example, we have

$$\begin{aligned} v_{\Delta}(t) &\simeq \mathbf{Z}\{i(t)\} + \int_0^T \frac{\partial v(t)}{\partial i(\tau)} \Delta i(\tau) d\tau \\ &= v(t) + \Delta v(t); \quad 0 \leq t < T \end{aligned}$$

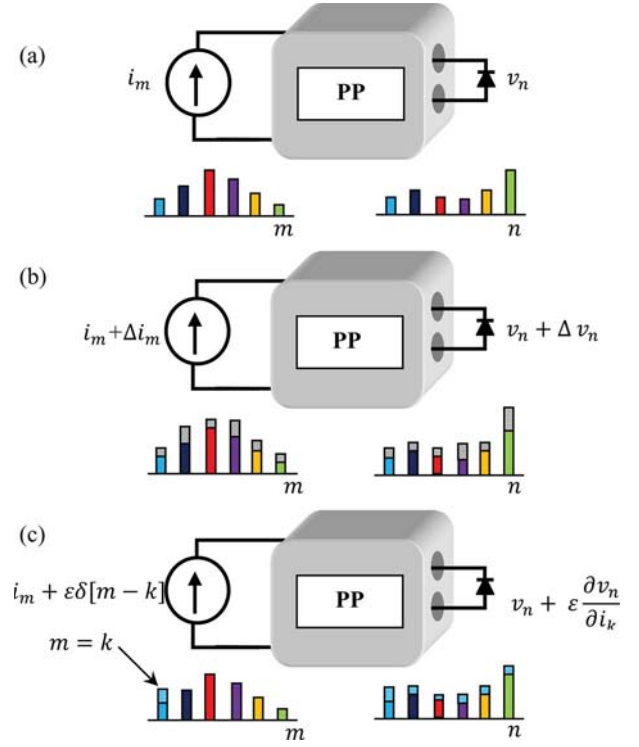


Fig. 4. Harmonic coupling in periodicity preservation systems.

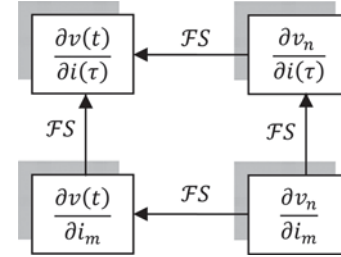


Fig. 5. The four Jacobians in terms of time and Fourier series coefficients for PP systems. The notation DFS denotes Fourier series—the synthesizing of continuous time periodic signals from their Fourier series coefficients.

so that (3) becomes

$$\Delta v(t) = \int_0^T \frac{\partial v(t)}{\partial i(\tau)} \Delta i(\tau) d\tau; \quad 0 \leq t < T. \quad (18)$$

Akin to (3) and (6) through (8), we summarize the affine PP approximations for estimating the output perturbations as a function of the input perturbations.

$$\Delta v(t) = \int_0^T \frac{\partial v(t)}{\partial i(\tau)} \Delta i(t) d\tau \Pi_T(t) \quad (19)$$

$$= \sum_{m=-\infty}^{\infty} \frac{\partial v(t)}{\partial i_m} \Delta i_m \Pi_T(t) \quad (20)$$

$$\Delta v_n = \int_0^T \frac{\partial v_n}{\partial i(\tau)} \Delta i(t) d\tau \quad (21)$$

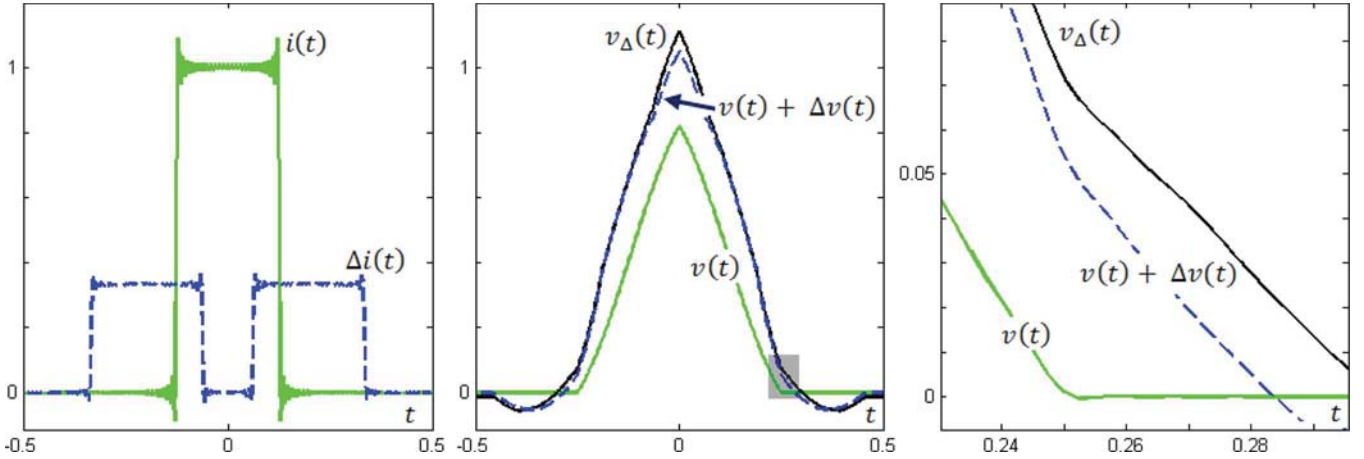


Fig. 6. A specific instance of Example 3 using the nonlinearity in (23). Both the input,  $i(t)$ , and perturbation  $\Delta i(t)$ , over a single period are the square waves shown on the left for 100 harmonics, i.e., using  $\{i_m\} - 100 \leq m \leq 100$ . The unperturbed output of TIPP system,  $v(t)$ , is shown in the middle plot. The perturbed output,  $v_\Delta(t)$  and the affine approximation,  $v(t) + \Delta v(t)$ , is shown in the middle figure. On the right is a close up of the shaded area in the middle plots. In all cases, 100 harmonics are used.

$$= \sum_{m=-\infty}^{\infty} \frac{\partial v_n}{\partial i_m} \Delta i_m. \quad (22)$$

Likewise, akin to Fig. 1, the relations among the Jacobians are shown in Fig. 5. Rather than Fourier transforms, the Jacobians are related by Fourier series relationships as in (14) and (15). Equations (20) through (22) and the entries in Fig. 5 are derived in Appendix C.

Of specific interest is (22) which is the linearization of the harmonic coupling of the perturbation. A small perturbation on the harmonic  $\Delta i_m$  makes contributions to all the response harmonics,  $\Delta v_n$ . The coupling is given by the Jacobian  $(\partial v_n)/(\partial i_m)$ . These are the *harmonic coupling weights* (HCWs). S-functions [16]–[20] and X-parameters [28]–[39] are HCWs.

The most straightforward approach to estimate the HCWs is shown in Fig. 4(c). The input is perturbed with a small amplitude *tickle tone*  $\Delta i_k$  at the  $k$ th input harmonic. In general, all of the output harmonics are perturbed from  $v_n$  to  $v_n + \Delta v_n$ . The ratio of the response perturbations to the stimulus perturbation can be used to estimate the HCWs  $(\partial v_n)/(\partial i_k) \simeq (\Delta v_n)/(\Delta i_k)$ . The experiment is repeated for different values of  $k$ .

Experimental methodologies for measuring HCWs is the topic of a forthcoming paper [67].

**Example 3: Mixed Squaring:** As an example of an affine approximation among Fourier series coefficients, consider the PP operation

$$v(t) = [2 \cos(2\pi t) i(t)]^2. \quad (23)$$

The Fourier coefficients are given by the convolution  $v_n = w_n * w_n$  where  $w_n = i_{n-1} - i_{n+1}$ . For a perturbation to  $i(t) + \Delta i(t)$ , the result is

$$\Delta v_n = 2(i_{n-1} - i_{n+1})(\Delta i_{n-1} - \Delta i_{n+1}).$$

A specific example is shown in Fig. 6. Details are in the caption.

**Theorem 3: Linear Systems:** For linear PP systems, the characterization in (19) through (22) are exact. The HCWs are given

by the impulse response of the (possibly time variant) linear system. Indeed, any linear system with impulse response  $h(t, \tau)$  can be made a PP system using

$$\frac{\partial v(t)}{\partial i(\tau)} = h(t, \tau) \Pi_T(\tau) \Pi_T(t) \quad (24)$$

where  $\Pi_T(\xi) = 1$  for  $0 \leq \xi < T$  and is zero otherwise.

The proof is in Appendix D.

**Theorem 4: Memoryless Nonlinearities:** A special class of PP systems is characterized by a memoryless nonlinearity (see (19))

$$v(t) = g(i(t)). \quad (25)$$

Then the harmonic coupling weights are

$$\frac{\partial v_n}{\partial i_m} = \vartheta_{n-m} \quad (26)$$

where  $\vartheta_n$  is the Fourier series coefficient of the periodic signal  $\dot{g}(i(t))$ .

$$\vartheta_n = \frac{1}{T} \int_0^T \dot{g}(i(t)) e^{-j2\pi n t/T} dt. \quad (27)$$

A proof is in Appendix E.

As a consequence of Theorem 4, *the harmonic coupling from a memoryless nonlinearity can always be expressed as a discrete convolution of Fourier series coefficients*. Substituting (26) into (22) gives

$$\Delta v_n = \sum_{m=-\infty}^{\infty} \vartheta_{n-m} \Delta i_m = \vartheta_n * \Delta i_n$$

and the asterisk denotes the discrete convolution operator. In the time domain, this is the same as the relationship in (11) when signals are periodic.

The Jacobian represented by (26) is Toeplitz. Knowledge of one row of the corresponding matrix for  $m = 0$ , i.e.,  $\vartheta_n$ , suffices to specify the entire Jacobian. This is of specific significance when the HCWs are determined experimentally. *Determination*

of a single row (or column) of the Jacobian HCWs of a memory-less nonlinearity allows specification of all HCWs. The required number of experiments is therefore significantly reduced.

## V. NONANALYTICITY

An implicit assumption thus far is that the different manifestations of the signals and systems are analytic. In terms of the Fourier coefficients, the stimulus can be expressed in terms of  $i_m$  and does not require use of the conjugate,  $i_m^*$ . The necessity of consideration of the analyticity of PP type operators in affine approximations is well known [20], [62]. Harmonic coupling, however, never requires nonanalytic treatment when the underlying signals and systems are real.

There are common PP operators that are not analytic, for example  $v(t) = |i(t)|^2$ . The relationship in the Fourier domain in this case is the correlation [52]

$$v_n = \sum_{k=-\infty}^{\infty} i_k^* i_{n+k}. \quad (28)$$

To generalize to such cases, Wirtinger calculus [64]–[66] can be used. The formalism emerging from Wirtinger calculus is that a variable and its conjugate, i.e.,  $i_m$  and  $i_m^*$ , are treated as separate variables. In lieu of approximation in (22), for example, Wirtinger calculus uses Jacobians of the form

$$\Delta v_n = \sum_{m=-\infty}^{\infty} \left( \frac{\partial v_n}{\partial i_m} \Delta i_m + \frac{\partial v_n}{\partial i_m^*} \Delta i_m^* \right). \quad (29)$$

From (28), for example,  $(\partial v_n)/(\partial i_m) = i_{m+n}^*$  and  $(\partial v_n)/(\partial i_m^*) = i_{m-n}$ .

When not a function of the conjugate,  $i_n^*$ , the second term in (29) is zero and (29) becomes the conventional HCW relationship in (22).

However, *when signals are real any expression that contains conjugate terms in the stimuli can be rearranged to not include conjugate terms. As a consequence, analyticity is assured and the use of Wirtinger calculus is never required.* If a periodic signal is real, its Fourier series coefficients are conjugately symmetric. For real  $\Delta i(t)$ , then, [52]

$$\Delta i_{-m} = \Delta i_m^*. \quad (30)$$

Any conjugate component in a series expression can be removed using this relationship. When  $i(t)$  is real, for example, (28) can be written without the use of the conjugate as  $v_n = \sum_{k=-\infty}^{\infty} i_{-k} i_{n+k}$ . In this form  $(\partial v_n)/(\partial i_m) = 2i_{n-m}$  and  $(\partial v_n)/(\partial i_m^*) = 0$ .

Likewise, *the conjugately symmetric property can be used to manipulate nonconjugate terms into conjugate terms in the case of real signals.* The Fourier series in (2) can be written as

$$\Delta v_n = \frac{\partial v_n}{\partial i_0} \Delta i_0 + \sum_{m=1}^{\infty} \frac{\partial v_n}{\partial i_m} \Delta i_m + \sum_{m=-\infty}^{-1} \frac{\partial v_n}{\partial i_m} \Delta i_m.$$

Reversing the summation order on the sum over negative arguments and using (30) gives

$$\Delta v_n = \frac{\partial v_n}{\partial i_0} \Delta i_0 + \sum_{m=1}^{\infty} \frac{\partial v_n}{\partial i_m} \Delta i_m + \sum_{m=1}^{\infty} \frac{\partial v_n}{\partial i_m^*} \Delta i_m^*.$$

Using this expression, the Jacobian expansions is no longer analytic and partials are required over conjugated variables. Wirtinger based relationships, for example, is used in X parameters [18], [24], [28]–[39]. For real signals and systems, however, the analytic expression in (22) suffices.

## VI. CONNECTIVITY AND OPERATIONS

The inversion of the impedance relationship  $v(t) = \mathbf{Z}\{i(t)\}$ , if it exists, is the admittance operator  $\mathbf{Y} = \mathbf{Z}^{-1}$  and

$$i(t) = \mathbf{Y}v(t).$$

A given  $\mathbf{Z}$  may not have a  $\mathbf{Y}$ , e.g., corresponding to  $v(t) = |i(t)|$ . Likewise, a given  $\mathbf{Y}$  may not have an inverse.

A dimensionless dependent source PP operator,  $\mathbf{G}$ , maps equivalent units, i.e.,  $i_2(t) = \mathbf{G}i_1(t)$  and  $v_2(t) = \mathbf{G}v_1(t)$ .

Consider the following connections.

- **Series.** If the same current,  $i(t)$ , passes through two TIPP operators,  $\mathbf{Z}_1$  and  $\mathbf{Z}_2$ , then the composite PP operator is  $\mathbf{Z} = \mathbf{Z}_1 + \mathbf{Z}_2$ .
- **Parallel.** Let  $v(t) = \mathbf{Z}_1 i_1(t)$ ,  $v(t) = \mathbf{Z}_2 i_2(t)$ . Let  $i(t) = i_1(t) + i_2(t) = [\mathbf{Z}_1^{-1} + \mathbf{Z}_2^{-1}]v(t)$  and, assuming all inverses exist,  $v(t) = \mathbf{Z}i(t)$  where  $\mathbf{Z} = [\mathbf{Z}_1^{-1} + \mathbf{Z}_2^{-1}]^{-1}$ .
- **Cascade.** Two PP operators  $\mathbf{Z}$  and  $\mathbf{G}$ , are in cascade when the composite operator,  $\mathbf{T}$ , is

$$\mathbf{T} = \mathbf{G}\mathbf{Z}. \quad (31)$$

PP generalizations of familiar circuit operations follow, including Kirchhoff's law and current and voltage dividers.

1) *Combining Cascade Operations:* Consider the cascade operation in (31). Let  $w(t) = \mathbf{Z}\{i(t)\}$ . Then

$$\Delta w(\xi) = \int_{-\infty}^{\infty} \frac{\partial w(\xi)}{\partial i(\tau)} \Delta i(\tau) d\tau.$$

Likewise, let  $v(t) = \mathbf{G}\{w(t)\}$ . Thus, the linearization of the Fourier series coefficients is

$$\begin{aligned} \Delta v(t) &= \int_{-\infty}^{\infty} \frac{\partial v(t)}{\partial w(\xi)} \Delta w(\xi) d\xi \\ &= \int_{-\infty}^{\infty} \frac{\partial v(t)}{\partial w(\xi)} \left( \int_{-\infty}^{\infty} \frac{\partial w(\xi)}{\partial i(\tau)} \Delta i(\tau) d\tau \right) d\xi \\ &= \int_{-\infty}^{\infty} \frac{\partial v(t)}{\partial i(\tau)} \Delta i(\tau) d\tau \end{aligned}$$

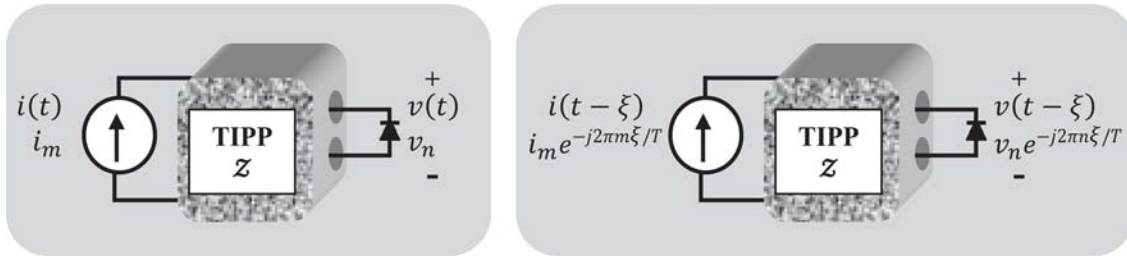


Fig. 7. On the left, an TIPPs system is stimulated by a sinusoidal source,  $i(t)$ . Its Fourier series coefficients are  $i_m$ . The response is  $v(t)$  with Fourier series coefficients  $v_n$ . Since the system is time invariant, an input shift of  $\xi$  results in the output being shifted by the same amount. As shown in the right hand figure, this corresponds to the Fourier series coefficients of both the stimulus and response being multiplied by the same exponential term.

where

$$\frac{\partial v(t)}{\partial i(\tau)} = \int_{-\infty}^{\infty} \frac{\partial v(t)}{\partial w(\xi)} \frac{\partial w(\xi)}{\partial i(\tau)} d\xi.$$

Similar relationships exist for the other forms of the Jacobian. For example, for harmonic coupling weights,

$$\frac{\partial v_n}{\partial i_m} = \sum_{k=-\infty}^{\infty} \frac{\partial v_n}{\partial w_k} \frac{\partial w_k}{\partial i_m}.$$

The HCW matrices of cascaded PP systems therefore multiply.

## VII. TIME INVARIANCE

If a system operator is time invariant, then any shift operator commutes with the  $\mathbf{Z}$  operator in (1). Thus, for all  $\xi$ , we have

$$\mathbf{Z}\{i(t - \xi)\} = v(t - \xi).$$

For any nonlinear system, from (3),

$$\Delta v(t - \xi) = \int_{-\infty}^{\infty} \frac{\partial v(t - \xi)}{\partial i(\tau - \xi)} \Delta i(\tau - \xi) d\tau. \quad (32)$$

For a time invariant system, the contribution of  $\partial i(t - \xi) dt$  at  $t = \tau + \xi$  to  $\partial v(t - \xi)$  is the same as the contribution of  $\partial i(t) dt$  at  $t = \tau$  to  $\partial v(t)$ . Thus,

$$\frac{\partial v(t - \xi)}{\partial i(\tau - \xi)} = \frac{\partial v(t)}{\partial i(\tau)}$$

and (32) becomes, for time invariant systems,

$$\Delta v(t - \xi) = \int_{-\infty}^{\infty} \frac{\partial v(t)}{\partial i(\tau)} \Delta i(\tau - \xi) d\tau.$$

The Jacobian for unshifted signals thus also works for shifted signals.

With reference to Fig. 7, Fourier transforming with respect to  $t$  gives

$$\Delta V(u) e^{-j2\pi u \xi} = \int_{-\infty}^{\infty} \frac{\partial V(u)}{\partial i(\tau)} \Delta i(\tau - \xi) d\tau.$$

Also with reference to Fig. 7, applying the power theorem of Fourier analysis [52] gives

$$\Delta V(u) e^{-j2\pi u \xi} = \int_{-\infty}^{\infty} \frac{\partial V(u)}{\partial I(\nu)} (\Delta I(\nu) e^{-j2\pi \nu \xi}) d\nu.$$

Perturbing the input spectrum by a linear phase factor therefore perturbs the response by the same factor.

For a time invariant periodic preservation (TIPPs) system, the analysis is similar. The harmonic coupling relationship in (22) generalizes, for all  $\xi$ , to

$$(\Delta v_n e^{-j2\pi n \xi / T}) = \sum_{m=-\infty}^{\infty} \frac{\partial v_n}{\partial i_m} (\Delta i_m e^{-j2\pi m \xi / T}).$$

Thus, when characterizing harmonic coupling in a TIPPs system, the HCWs for unshifted periodic inputs can be used to find the HCWs for all shifted versions of the input. Both the operating point and the perturbation are shifted by the same amount. This is illustrated in Fig. 6.

## VIII. EXTENSION TO MULTI-PORT SYSTEMS

The extension from one port systems to two or more ports is straightforward. Through our choice of notation in (1), the system stimulus is a current and the response is a voltage. The system mapping,  $\mathbf{Z}$  therefore has the same units as impedance can be spectrally characterized by stimulus with a series of sinusoids at different frequencies and noting the amplitude and phase shift of the response. The  $\mathbf{Z}$  mapping, however, is more general than an impedance allowing, of course, nonlinearities but also dependent and independent sources. The operator is not constrained by the homogeneity property of linearity [52]. A zero stimulus, for example, can yield a nonzero response. As an example of a familiar system that is not an impedance, consider a series  $RL$  circuit with an independent voltage source and a  $\mathbf{Z}$  mapping that can be written as

$$v(t) = \mathbf{Z}(i(t)) = Ri(t) + L \frac{di(t)}{dt} + v_0(t) \quad (33)$$

or, in the Fourier domain

$$V(u) = (R + j2\pi uL)I(u) + V_0(u).$$

Impedance is defined as the ratio between a voltage and a current phasor. Due to inclusion of the independent voltage source,

$v_0(t)$ , the ratio  $V(u)/I(u)$  is not meaningful for this  $\mathbf{Z}$ . Indeed,  $\mathbf{Z}$  cannot be conventionally characterized by an impulse response. A sinusoidal stimulus does not generally result in a sinusoidal response due to the independent voltage source. In this sense, spectral characterization of  $\mathbf{Z}$  through mapping of response amplitude and phase variation to stimuli at various frequencies will also not work. If, however,  $v_0(t)$  is periodic, then  $\mathbf{Z}$  is PP for periodic stimuli with the same period. Although not necessarily the best way, the system can be accurately characterized using HCW's.

The characterization of PP systems is similar to LTI except generalized to measuring coupling weights across the harmonic spectrum for varying input tones of various frequencies. For a loaded two port, the cross port parameters are still characterized by a  $\mathbf{Z}$  mapping albeit the stimulus and response are not at the same ports.

Reformulating HCW's applied to circuits from current stimuli to voltage stimuli or dimensionless stimuli is also straightforward.

## IX. CONCLUSION

We have shown the following.

- A class of systems, dubbed periodicity preservation (PP) systems, can be characterized for small stimulus perturbation using harmonic coupling weights (HCWs). The characterization requires no model of the PP system.
- PP operations include addition, filtering, memoryless nonlinearity, shift, and mixing (multiplication).
- For linear and possibly time variant PP systems, the approximation of harmonic coupling weights gives exact results.
- Cascade, series and parallel connections of PP operations result in a composite PP system. The composite harmonic coupling weights can be determined directly from the components' harmonic coupling weights.
- As LTI systems require a single stimulus-response pair for complete characterization (e.g., the impulse response), memoryless nonlinearity PP systems require only a single stimulus-response characterization. Other PP systems typically require more.
- Any PP system with real stimuli and responses can be characterized without the use of Wirtinger calculus. Conversely, taking advantage of the conjugate symmetry of Fourier series coefficients of real signals, the harmonic coupling weights can be placed in a form using Wirtinger calculus.
- For a time invariant PP (TIPP) system, the complex exponential weighting invoked on input Fourier coefficients results in the exact same weighting on the output Fourier coefficients. Thus, for example, the TIPP characterization for a cosine stimulus operating point can be used to evaluate the harmonic coupling weights for the same system if the operating point were a sine.
- The HCWs corresponding to memoryless TIPP systems display Toeplitz symmetry.

The PP systems are a useful type system class that includes nonlinearities commonly encountered in practice, especially in

nonlinear engineering circuit and system design. Both time-domain and Fourier-domain affine approximations can be used to model the behavior of certain PP systems. PP and TIPP systems show promise for modeling large classes of nonlinearities in many circuit design problems and nonlinear applications in other engineering disciplines.

## APPENDIX

### A. Derivation of the Entries in Fig. 1

The Fourier transform of  $i(t)$  is  $I(u)$ .

$$i(\tau) = \int_{-\infty}^{\infty} I(u) e^{j2\pi u\tau} du. \quad (\text{A1})$$

Setting

$$\frac{\partial I(u)}{\partial I(v)} = \delta(v - u) \quad (\text{A2})$$

we have using (A1)

$$\frac{\partial i(\tau)}{\partial I(v)} = \int_{-\infty}^{\infty} \frac{\partial I(u)}{\partial I(v)} e^{j2\pi u\tau} du = e^{j2\pi v\tau}.$$

Then

$$\frac{\partial v(t)}{\partial I(v)} = \int_{-\infty}^{\infty} \frac{\partial v(t)}{\partial i(\tau)} \frac{\partial i(\tau)}{\partial I(v)} d\tau = \int_{-\infty}^{\infty} \frac{\partial v(t)}{\partial i(\tau)} e^{j2\pi v\tau} dt. \quad (\text{A3})$$

This corresponds to the leftmost vertical arrow in Fig. 1. Typically, a negative sign is on the exponent of the time to frequency Fourier transformation. This is not the case here, so the arrow points up.

Using (A3) we can write, in lieu of (3)

$$\Delta v(t) = \int_{-\infty}^{\infty} \frac{\partial v(t)}{\partial I(v)} \Delta I(v) dv. \quad (\text{A4})$$

This is (6).

From (4)

$$\frac{\partial V(u)}{\partial v(t)} = e^{-j2\pi ut}. \quad (\text{A5})$$

Fourier transforming  $(\partial v(t))/(\partial i(\tau))$  gives

$$\int_{-\infty}^{\infty} \frac{\partial v(t)}{\partial i(\tau)} e^{-j2\pi ut} dt = \int_{-\infty}^{\infty} \frac{\partial v(t)}{\partial i(\tau)} \frac{\partial V(u)}{\partial v(t)} dt = \frac{\partial V(u)}{\partial i(\tau)}.$$

Therefore,  $(\partial v(t))/(\partial i(\tau))$  and  $(\partial V(u))/(\partial i(\tau))$  are Fourier transform pairs as depicted in the top horizontal arrow in Fig. 1. We then Fourier transform both sides of (3) to obtain (7)

$$\begin{aligned} \Delta V(u) &= \int_{-\infty}^{\infty} \left[ \int_{-\infty}^{\infty} \frac{\partial v(t)}{\partial i(\tau)} e^{-j2\pi ut} dt \right] \Delta i(\tau) d\tau \\ &= \int_{-\infty}^{\infty} \frac{\partial V(u)}{\partial i(\tau)} \Delta i(\tau) d\tau. \end{aligned}$$

Applying (A5) to the Fourier transform of  $(\partial v(t))/(\partial I(\nu))$  gives

$$\int_{-\infty}^{\infty} \frac{\partial v(t)}{\partial I(\nu)} e^{-j2\pi ut} dt = \int_{-\infty}^{\infty} \frac{\partial v(t)}{\partial I(\nu)} \frac{\partial V(u)}{\partial v(t)} dt = \frac{\partial V(u)}{\partial I(\nu)}.$$

This corresponds to the bottom horizontal arrow in Fig. 1. Fourier transforming both sides of (A4) then gives (8).

Lastly, consider the Fourier transform

$$\int_{-\infty}^{\infty} \frac{\partial V(u)}{\partial I(\nu)} e^{-j2\pi\nu\tau} d\nu = \int_{-\infty}^{\infty} \frac{\partial V(u)}{\partial I(\nu)} \frac{\partial I(\nu)}{\partial i(\tau)} d\nu = \frac{\partial V(u)}{\partial i(\tau)}.$$

This relationship corresponds to the rightmost vertical arrow in Fig. 1.

### B. Proof of Theorem 1

A linear system can be expressed as the superposition integral [52]

$$v(t) = \int_{-\infty}^{\infty} i(\tau)h(t, \tau) d\tau$$

where  $h(t, \tau)$  is the impulse response of the system,  $h(t, \tau) = \mathbf{Z}\{\delta(t - \tau)\}$ . Thus,

$$\frac{\partial v(t)}{\partial i(\tau)} = h(t, \tau).$$

Therefore, we have the equality

$$\begin{aligned} \mathbf{Z}\{i(\tau) + \Delta i(\tau)\} &= \int_{-\infty}^{\infty} (i(\tau) + \Delta i(\tau))h(t, \tau) d\tau \\ &= v(t) + \Delta v(t) \end{aligned}$$

where  $\Delta v(t)$  is given by precisely by

$$\Delta v(t) = \mathbf{Z}\{\Delta i(t)\} = \int_{-\infty}^{\infty} \Delta i(\tau)h(t, \tau) d\tau.$$

### C. Derivation of the Entries in Fig. 5

The operating point input can be expressed by the Fourier series

$$i(\tau) = \sum_{k=-\infty}^{\infty} i_k e^{j2\pi k\tau/T} \Pi_T(t)$$

so that

$$\frac{\partial i(\tau)}{\partial i_m} = e^{j2\pi m\tau/T} \Pi_T(\tau). \quad (\text{A6})$$

Using the Fourier series expansion of  $\Delta i(\tau)$ , (18) can be written as

$$\Delta v(t) = \int_{-\infty}^{\infty} \frac{\partial v(t)}{\partial i(\tau)} \left[ \sum_{m=-\infty}^{\infty} \Delta i_m e^{j2\pi m\tau/T} \Pi_T(\tau) \right] d\tau$$

$$= \sum_{m=-\infty}^{\infty} \left[ \int_{-\infty}^{\infty} \frac{\partial v(t)}{\partial i(\tau)} e^{j2\pi m\tau/T} \Pi_T(\tau) d\tau \right] \Delta i_m. \quad (\text{A7})$$

But, using (A6), we have

$$\begin{aligned} \int_{-\infty}^{\infty} \frac{\partial v(t)}{\partial i(\tau)} e^{j2\pi m\tau/T} \Pi_T(\tau) d\tau &= \int_{-\infty}^{\infty} \frac{\partial v(t)}{\partial i(\tau)} \frac{\partial i(\tau)}{\partial i_m} d\tau \\ &= \frac{\partial v(t)}{\partial i_m}. \end{aligned}$$

This corresponds to the upper horizontal arrow in Fig. 5 and, when substituted into (A7), we obtain (20).

The Fourier series coefficients for the output operating point are

$$\begin{aligned} v_n &= \frac{1}{T} \int_0^T v(t) e^{-j2\pi nt/T} dt \\ &= \frac{1}{T} \int_{-\infty}^{\infty} v(\xi) e^{-j2\pi n\xi/T} \Pi_T(\xi) d\xi \end{aligned}$$

so that

$$\frac{\partial v_n}{\partial v(t)} = \frac{1}{T} e^{-j2\pi nt/T} \Pi_T(t). \quad (\text{A8})$$

Likewise, the Fourier series coefficients of the output perturbation are

$$\Delta v_n = \frac{1}{T} \int_{-\infty}^{\infty} \Delta v(t) e^{-j2\pi nt/T} \Pi_T(t) dt.$$

Using (20)

$$\begin{aligned} \Delta v_n &= \frac{1}{T} \int_{-\infty}^{\infty} \left[ \sum_{m=-\infty}^{\infty} \frac{\partial v(t)}{\partial i_m} \Delta i_m \right] e^{-j2\pi nt/T} \Pi_T(t) dt \\ &= \sum_{m=-\infty}^{\infty} \int_{-\infty}^{\infty} \left[ \frac{\partial v(t)}{\partial i_m} \left( \frac{1}{T} e^{-j2\pi nt/T} \Pi_T(t) \right) \right] dt \Delta i_m. \end{aligned}$$

Substituting (A8)

$$\begin{aligned} \Delta v_n &= \sum_{m=-\infty}^{\infty} \int_{-\infty}^{\infty} \left[ \frac{\partial v(t)}{\partial i_m} \frac{\partial v_n}{\partial v(t)} \right] dt \Delta i_m \\ &= \sum_{m=-\infty}^{\infty} \frac{\partial v_n}{\partial i_m} \Delta i_m. \end{aligned}$$

This is the expression describing harmonic coupling.

### D. Proof of Theorem 3

A PP system is linear if

$$v(t) = \int_{-\infty}^{\infty} i(\tau)h(t, \tau)\Pi_T(\tau) d\tau \Pi_T(t).$$

Thus

$$\frac{\partial v(t)}{\partial i(\tau)} = h(t, \tau) \Pi_T(\tau) \Pi_T(t)$$

and the response to a perturbed operating point is

$$\begin{aligned} v_{\Delta}(t) &= \int_{-\infty}^{\infty} (i(\tau) + \Delta i(\tau)) h(t, \tau) \Pi_T(\tau) d\tau \Pi_T(t) \\ &= v(t) + \Delta v(t) \end{aligned}$$

where  $\Delta v(t)$  is given by (19). Equations (20)–(22) are alternate descriptions of the same identity.

#### E. Proof of Theorem 4

Given (25), the response Fourier series coefficient is

$$\begin{aligned} v_n &= \frac{1}{T} \int_{-\infty}^{\infty} g(i(t)) e^{-j2\pi nt/T} \Pi_T(t) dt \\ &= \frac{1}{T} \int_{-\infty}^{\infty} g \left( \sum_{k=-\infty}^{\infty} i_k e^{j2\pi kt/T} \Pi_T(t) \right) e^{-j2\pi nt/T} \Pi_T(t) dt. \end{aligned}$$

Therefore from the chain rule of differentiation

$$\begin{aligned} \frac{\partial v_n}{\partial i_m} &= \frac{1}{T} \int_{-\infty}^{\infty} \dot{g} \left( \sum_{k=-\infty}^{\infty} i_k e^{j2\pi kt/T} \Pi_T(t) \right) \\ &\quad \times e^{-j2\pi(n-m)t/T} \Pi_T(t) dt \\ &= \frac{1}{T} \int_{-\infty}^{\infty} \dot{g}(i(t)) e^{-j2\pi(n-m)t/T} \Pi_T(t) dt = \vartheta_{n-m} \end{aligned}$$

where  $\vartheta_n$  is defined in (27).

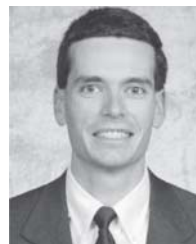
#### ACKNOWLEDGMENT

The authors would like to express appreciation to L. Cohen, J. de Graaf, and Dr. E. Mokole of NRL for their technical expertise and advice throughout this research. The contributions of Baylor student research assistants J. Martin and M. Moldovan are greatly appreciated. The authors also thank the reviewers and the Associate Editor for one of the most in-depth and helpful review processes we have ever experienced. The paper is of higher quality because of their efforts.

#### REFERENCES

- [1] H. Sira-Ramirez, P. Lischinsky-Arenas, and O. Llanes-Santiago, "Dynamic compensator design in nonlinear aerospace systems," *IEEE Trans. Aerosp. Electron. Syst.*, vol. 29, no. 2, pp. 364–379, Apr. 1993.
- [2] K. J. Karimi and A. C. Mong, "Modeling nonlinear loads for aerospace power systems," in *Proc. IECEC'02. 2002 37th Intersociety*, Jul. 29–31, 2004, pp. 33–38.
- [3] J. Sun, M. Chen, and K. J. Karimi, "Aircraft power system harmonics involving single-phase PFC converters," *IEEE Trans. Aerosp. Electron. Syst.*, vol. 44, no. 1, pp. 217–226, Jan. 2008.
- [4] M. Brooker and M. Inggs, "A signal level simulator for multistatic and netted radar systems," *IEEE Trans. Aerosp. Electron. Syst.*, vol. 47, no. 1, pp. 178–186, Jan. 2011, doi: 10.1109/TAES.2011.5705668.
- [5] M. V. Campos and M. Silveira, "An efficient analytical approach for the nonlinear analysis of RF amplifiers implemented with the FET structures," in *Proc. APMC 2005*, Dec. 4–7, 2005, vol. 1, p. 4.
- [6] C.-S. Chiu, S.-Y. Lin, B.-Y. Chen, K.-M. Chen, and G.-W. Huang, "Nonlinear behavior characterization of RF active devices using impedance-dependence X-parameters," in *Proc. APMC 2010*, Dec. 7–10, 2010, pp. 2307–2310.
- [7] C. Baylis, R. J. Marks, II, J. Martin, H. Miller, and M. Moldovan, "Going nonlinear," *IEEE Microw. Mag.*, pp. 55–64, Apr. 2011.
- [8] J. de Graaf, H. Faust, J. Alatishe, and S. Talapatra, "Generation of spectrally confined transmitted radar waveforms," in *Proc. IEEE Conf. Radar*, 2006, pp. 76–83.
- [9] K. J. Karimi and A. C. Mong, "Modeling nonlinear loads for aerospace power systems," in *Proc. IECEC'02. 2002 37th Intersociety*, Jul. 29–31, 2004, pp. 33–38.
- [10] J. C. Pedro and N. B. Carvalho, *Intermodulation Distortion in Microwave and Wireless Circuits*. Norwood, MA: Artech House, 2003, pp. 21–22, 29–30.
- [11] L. Betts, "Vector and harmonic amplitude/phase corrected multi-envelope response measurements of nonlinear devices," in *Proc. IEEE MTT-S International Microwave Symp.*, 2008, pp. 261–264.
- [12] M. Isaksson *et al.*, "A comparative analysis of behavioral models for RF power amplifiers," *IEEE Trans. Microw. Theory Tech.*, vol. 54, no. 1, pp. 348–359, Jan. 2006.
- [13] J. A. Jargon, K. C. Gupta, and D. C. DeGroot, "Nonlinear large-signal scattering parameters: Theory and application," in *63rd ARFTG Microwave Measurement Conf. Dig.*, Jun. 2004, pp. 157–174.
- [14] J. C. Pedro *et al.*, "A comparative overview of microwave and wireless power-amplifier behavioral modeling approaches," *IEEE Trans. Microw. Theory Tech.*, vol. 53, no. 4, Apr. 2005.
- [15] J. Wood and D. E. Root, *Fundamentals of Nonlinear Behavioral Modeling for RF and Microwave Design*. Norwood, MA: Artech House, 2005, ch. 3.
- [16] F. Verbeyst and M. Vanden Bossche, "VIOMAP, the S-parameter equivalent for weakly nonlinear RF and microwave devices," *IEEE Trans. Microw. Theory Tech.*, vol. 42, no. 12, pp. 2531–2535, Dec. 1994.
- [17] M. Myslinski, F. F. Verbeyst, M. B. Vanden, and D. Schreurs, "A method to select correct stimuli levels for S-functions behavioral model extraction," in *Proc. IEEE MTT-S Int.*, May 23–28, 2010, pp. 1–1, doi: 10.1109/MWSYM.2010.5518233.
- [18] G. Sun, Y. Xu, and A. Liang, "The study of nonlinear scattering functions and X-parameters," in *Proc. ICMMT*, 2010, pp. 1086–1089, DOI: 10.1109/ICMMT.2010.5525111.
- [19] J. Verspecht, M. Vanden Bossche, and F. Verbeyst, "Characterizing components under large signal excitation: Defining sensible 'large signal S-parameters'," in *Proc. 49th ARFTG Conf. Dig.*, 1997, pp. 109–117.
- [20] J. Verspecht, D. F. Williams, D. Schreurs, K. A. Remley, and M. D. McKinley, "Linearization of large-signal scattering functions," *IEEE Trans. Microw. Theory Tech.*, vol. 53, no. 4, pp. 1369–1376, Apr. 2005.
- [21] J. Verspecht, J. Horn, and D. E. Root, "A simplified extension of X-parameters to describe memory effects for wideband modulated signals," in *Proc. ARFTG*, May 28–28, 2010, pp. 1–6, doi: 10.1109/ARFTG.2010.5496334.
- [22] C.-S. Chiu, K.-M. Chen, G.-W. Huang, C.-H. Hsiao, K.-H. Liao, W.-L. Chen, S.-C. Wang, M.-Y. Chen, Y.-C. Yang, K.-L. Wang, and L.-K. Wu, "Characterization of annular-structure RF LD MOS transistors using polyharmonic distortion model," in *Proc. IEEE MTT-S Int. Microw. Symp. Dig.*, pp. 977–980, DOI: 10.1109/MWSYM.2009.5165862.
- [23] C.-S. Chiu, S.-Y. Lin, B.-Y. Chen, K.-M. Chen, and G.-W. Huang, "Nonlinear behavior characterization of RF active devices using impedance-dependence X-parameters," in *Proc. APMC*, Dec. 7–10, 2010, pp. 2307–2310.
- [24] C.-S. Chiu, K.-M. Chen, G.-W. Huang, S.-Y. Lin, B.-Y. Chen, C.-C. Hung, S.-Y. Huang, C.-W. Fan, C.-Y. Tzeng, and S. Chou, "Power improvement for 65 nm nMOSFET with high-tensile CESL and fast nonlinear behavior modeling," in *Proc. 2010 IEEE RFIC*, pp. 589–592, DOI: 10.1109/RFIC.2010.5477258.

- [25] D. E. Root, J. Verspecht, D. Sharrit, J. Wood, and A. Cognata, "Broadband polyharmonic distortion (PHD) behavioral models from fast automated simulations and large-signal vectorial network measurements," *IEEE Trans. Microw. Theory*, vol. 53, no. 11, pp. 3656–3664, Nov. 2005.
- [26] R. S. Saini, S. Woodington, J. Lees, J. Benedikt, and P. J. Tasker, "An intelligence driven active loadpull system," in *Proc. 2010 75th ARFTG*, pp. 1–4, DOI: 10.1109/ARFTG.2010.5496327.
- [27] J. Verspecht *et al.*, "Multi-port, and dynamic memory enhancements to PHD nonlinear behavioral models from large-signal measurements and simulations," in *Proc. Conf. Rec. IEEE Microw. Theory Tech. Symp. 2007*, Jun. 2007, pp. 969–972.
- [28] D. T. Bepalko and S. Boumaiza, "X-parameter measurement challenges for unmatched device characterization," in *Proc. 2010 75th ARFTG*, pp. 1–4, DOI: 10.1109/ARFTG.2010.5496317.
- [29] D. Gunyan, J. Horn, J. Xu, and D. E. Root, "Nonlinear validation of arbitrary load X-parameter and measurement-based device models," in *Proc. 2009 73rd ARFTG*, pp. 1–4, DOI: 10.1109/ARFTG.2009.5278063.
- [30] J. M. Horn, J. Verspecht, D. Gunyan, L. Betts, D. E. Root, and J. Eriksson, "X-parameter measurement and simulation of a GSM handset amplifier," in *Proc. 2 EuMIC 2008*, pp. 135–138, DOI: 10.1109/EMICC.2008.477224.
- [31] Horn, L. Betts, C. Gillease, J. Verspecht, D. Gunyan, and D. E. Root, "Measurement-based large-signal simulation of active components from automated nonlinear vector network analyzer data via X-parameters," in *Proc. COMCAS*, 2008, pp. 1–6, DOI: 10.1109/COMCAS.2008.4562819.
- [32] J. Horn, D. E. Root, and G. Simpson, "GaN device modeling with X-parameters," in *Proc. 2010 IEEE CSICS*, pp. 1–4, DOI: 10.1109/CSICS.2010.561969.
- [33] J. Randa, "Uncertainty analysis for noise-parameter measurements," in *Proc. Conf. Precision Electromagn. Measurements Dig.*, 2008, pp. 498–499, DOI: 10.1109/CPEM.2008.4574871.
- [34] D. E. Root, J. Xu, J. Horn, M. Iwamoto, and G. Simpson, "Device modeling with NVNAs and X-parameters," in *Proc. 2010 Workshop INMMIC*, pp. 12–15, DOI: 10.1109/INMMIC.2010.5480151.
- [35] G. Simpson, J. Horn, D. Gunyan, and D. E. Root, "Load-pull + NVNA = enhanced X-parameters for PA designs with high mismatch and technology-independent large-signal device models," in *Proc. 72nd ARFTG*, 2008, pp. 88–91, DOI: 10.1109/ARFTG.2008.4804301.
- [36] G. Simpson, "High power load pull with X-parameters—A new paradigm for modeling and design," in *Proc. IEEE 11th Ann. WAMICON*, 2010, pp. 1–4, doi: 10.1109/WAMICON.2010.5461843.
- [37] M. S. Taci and I. Doseyn, "Determining the harmonic components of nonlinear impedance loads in terms of resistances and reactances by using a current harmonic method," in *Proc. MELECON'98. 9th Mediterranean Electrotechnical Conf.*, 1998, vol. 2, pp. 1000–1003, DOI: 10.1109/MELCON.1998.699379.
- [38] J. Verspecht, J. Horn, L. Betts, D. Gunyan, R. Pollard, C. Gillease, and D. E. Root, "Extension of X-parameters to include long-term dynamic memory effects," in *Proc. 2009 IEEE Int. Microw. Symp.*, Boston, MA, pp. 741–744.
- [39] J. Wood and G. Collins, "Investigation of X-parameters measurements on a 100 W Doherty power amplifier," in *Proc. 75th ARFTG*, 2010, pp. 1–7, DOI: 10.1109/ARFTG.2010.5496319.
- [40] M. Schetzen, *The Volterra and Wiener Theories of Nonlinear Systems*, Revised ed. Malabar, FL: Krieger Publishing Company, 2006.
- [41] K. S. Shanmugam and M. T. Jong, "Identification of nonlinear systems in frequency domain," *IEEE Trans. Aerosp. Electron. Syst.*, vol. AES-11, no. 6, pp. 1218–1225, Nov. 1975, doi: 10.1109/TAES.1975.308179.
- [42] S. Benedetto, E. Biglieri, and R. Daffara, "Modeling and performance evaluation of nonlinear satellite links—A Volterra series approach," *IEEE Trans. Aerosp. Electron. Syst.*, vol. AES-15, no. 4, pp. 494–507, Jul. 1979, doi: 10.1109/TAES.1979.308734.
- [43] S. A. Maas, *Nonlinear Microwave and RF Circuits*, 2nd ed. Norwood, MA: Artech House, 2003.
- [44] A. Zhu, T. Wang, and T. J. Brazil, "Narrowband and Volterra-based behavioral models of high frequency amplifiers," in *Proc. 58th ARFTG Conf. Digest-Fall*, Nov. 2001, vol. 40, pp. 1–9.
- [45] D. Mirri, G. Iuculano, F. Ilicori, G. Pasini, G. Vannini, and G. Pellegrini, "A modified Volterra series approach for nonlinear dynamic system modeling," *IEEE Trans. Circuits Syst. I, Analog Digit. Signal Process.*, vol. 49, no. 8, pp. 1118–1128, Aug. 2002.
- [46] J. B. Thomas, *Introduction to Statistical Communication Theory*. New York: Wiley, 1969.
- [47] R. L. Boylestad, *Introductory Circuit Analysis*, 12th ed. Englewood Cliffs, NJ: Prentice Hall, 2010.
- [48] P. L. Heron and M. B. Steer, "Jacobian calculation using the multidimensional fast Fourier transform in the harmonic balance analysis of nonlinear circuits," *IEEE Trans. Microw. Theory Tech.*, vol. 38, no. 4, pp. 429–431, Apr. 1990.
- [49] S. Jahanbakht and F. Farzaneh, "Computing all the Floquet eigenfunctions of oscillators using harmonic balance Jacobian matrices," *Circuits, Devices & Systems, IET*, vol. 5, no. 4, pp. 257–266, Jul. 2011.
- [50] R. J. Marks, II, J. F. Walkup, and M. O. Hagler, "Methods of linear system characterization through response cataloging," *Appl. Opt.*, vol. 18, pp. 655–659, 1979.
- [51] R. J. Marks, II, I. A. Gravagne, J. M. Davis, and J. J. DaCunha, "Nonregressivity in switched linear circuits and mechanical systems," *Mathematical Computer Modelling*, vol. 43, no. 11, pp. 1383–1392, 2012.
- [52] R. J. Marks, II, *Handbook of Fourier Analysis and Its Applications*. Oxford, U.K.: Oxford University Press, 2009.
- [53] R. J. Marks, II, "Sampling theory for linear integral transforms," *Opt. Lett.*, vol. 6, pp. 7–9, 1981.
- [54] R. J. Marks, II, J. F. Walkup, and M. O. Hagler, "A sampling theorem for space-variant systems," *J. Opt. Soc. Amer.*, vol. 66, no. 9, pp. 918–921, 1976.
- [55] R. J. Marks, II, J. F. Walkup, M. O. Hagler, and T. F. Krile, "Space-variant processing of one-dimensional signals," *Appl. Opt.*, vol. 16, pp. 739–745, 1977.
- [56] T. F. Krile, R. J. Marks, II, J. F. Walkup, and M. O. Hagler, "Holographic representations of space-variant systems using phase-coded reference beams," *Appl. Opt.*, vol. 16, no. 12, pp. 3131–3135, 1977.
- [57] R. J. Marks, II, J. F. Walkup, and M. O. Hagler, "Sampling theorems for linear shift-variant systems," *IEEE Trans. Circuits Syst.*, vol. CAS-25, pp. 228–233, 1978.
- [58] J. M. Davis, I. A. Gravagne, and R. J. Marks, II, "Convergence of unilateral Laplace transforms on time scales," *Circuits, Systems, and Signal Processing*, vol. 29, no. 5, pp. 971–997, 2010.
- [59] J. M. Davis, I. A. Gravagne, and R. J. Marks, II, "Bilateral Laplace transforms on time scales: Convergence, convolution, and the characterization of stationary stochastic time series," *Circuits, Systems, and Signal Processing*, vol. 29, no. 6, pp. 1141–1165, 2010.
- [60] R. J. Marks, II and J. N. Larson, "One-dimensional Mellin transformation using a single optical element," *Appl. Opt.*, vol. 18, pp. 754–755, 1979.
- [61] R. J. Marks, II, I. A. Gravagne, and J. M. Davis, "A generalized Fourier transform and convolution on time scales," *J. Math. Anal. Appl.*, vol. 340, no. 2, pp. 901–919, Apr. 15, 2008.
- [62] J. Verspecht and D. Root, "Polyharmonic distortion modeling," *IEEE Microw. Mag.*, vol. 7, no. 3, pp. 44–57, Jun. 2006.
- [63] R. J. Marks, II, "Restoring lost samples from an oversampled bandlimited signal," *IEEE Trans. Acoustics, Speech Signal Process.*, vol. ASSP-31, no. 3, pp. 752–755, Jun. 1983.
- [64] W. Wirtinger, "Zur Formalen Theorie der Funktionen von mehr Complexen Veränderlichen," *Math. Ann.*, vol. 97, pp. 357–375, 1927.
- [65] R. F. H. Fischer, *Precoding and Signal Shaping for Digital Transmission*. New York: Wiley, 2005.
- [66] K. L. Du and M. N. S. Swamy, *Wireless Communication Systems From RF Subsystems to 4G Enabling Technologies*. Cambridge, U.K.: Cambridge Univ. Press, 2010.
- [67] C. Baylis and R. J. Marks, II, "Evaluation of harmonic coupling weights in nonlinear periodicity preservation systems," *IEEE Trans. Circuits Syst. I, Reg. Papers*, to be published.



**Charles Baylis, II** (S'03–M'08) received the D.Phil. in electrical engineering from the University of South Florida, Tampa, in May 2007.

He is Assistant Professor and the Co-Director of the Wireless and Microwave Circuits and Systems Program, Department of Electrical and Computer Engineering, Baylor University, Waco, TX. For 2007–2008 he was a Visiting Assistant Professor at Department of Electrical Engineering, University of South Florida, Tampa. He specializes in high-efficiency power amplifier design for radar

and communication systems, nonlinear microwave measurements, nonlinear transistor modeling techniques and approaches, related system applications.

Dr. Baylis was the General Chair of the First and Second Mini-Symposia on Wireless and Microwave Circuits and Systems, Waco, TX, April 2009 and March 2010. He serves on the executive Committee Member and Student Activities Chair of the IEEE Microwave Theory and Techniques Society, Dallas Chapter, 2009–2011.



**Robert J. Marks, II** (S'71–M'72–SM'83–F'94) is Distinguished Professor of Electrical and Computer Engineering, Baylor University, Waco, TX, consulting activities include Microsoft Corporation, Pacific Gas & Electric, and Boeing Computer Services.

His research has been funded by organizations such as the National Science Foundation, General Electric, Southern California Edison, EPRI, the Air Force Office of Scientific Research, the Office of Naval Research, the Whitaker Foundation, Boeing Defense, the National Institutes of Health, The Jet Propulsion Lab, Army Research Office, and NASA.

Prof. Marks is the recipient of numerous professional awards, including a NASA Tech Brief Award and a best paper award from the American Brachytherapy Society for prostate cancer research. He is Fellow of both IEEE and The Optical Society of America. He was awarded the IEEE Outstanding Branch Councilor Award, The IEEE Centennial Medal, the IEEE Neural Networks Society Meritorious Service Award, the IEEE Circuits and Systems Society Golden Jubilee Award and, for 2007, the IEEE CIS Chapter of the IEEE Dallas Section Volunteer of the Year award. He was named a Distinguished Young Alumnus of Rose-Hulman Institute of Technology, is an inductee into the Texas Tech Electrical Engineering Academy, and in 2007 was awarded the Banned Item of the Year from the Discovery Institute. Dr. Marks served for 17 years as the faculty advisor to the University of Washington's chapter of Campus Crusade for Christ. In 2010, he was listed by CollegeCrunch.com as one of "The 20 Most Brilliant Christian Professors".